Profile and clinical implication of circular RNAs in human papillary thyroid carcinoma

Huihui Ren [1] , **Zhelong Liu** [1] , **Siyue Liu** [1] , **Xinrong Zhou** [1] , **Hong Wang** [2] , **Jinchao Xu** [2] , **Daowen Wang** Corresp., [1,2] , **Gang Yuan** Corresp. [1]

[1] Department of Internal Medicine, Tongji Hospital, Huazhong University of Science and Technology, Wuhan, China

[2] Molecular Diagnostic Laboratory, Tongji Hospital, Huazhong University of Science and Technology, Wuhan, China

Corresponding Authors: Daowen Wang, Gang Yuan
Email address: dwwang@tjh.tjmu.edu.cn, gangyuan@tjh.tjmu.edu.cn

Background: Differently expressed circular RNAs (circRNAs) have been reported to play a considerable role in tumor behavior; however, the expression profile and biological function of circRNAs in papillary thyroid carcinoma (PTC) remains unknown. Thus, the study was aimed to characterize the circRNA expression profile to comprehensively understand the biological behavior of PTC. Methods : We investigated the expression profile of circRNAs using circRNA microarray in three pairs of PTC and adjacent normal tissues. Quantitative real-time reverse transcription polymerase chain reaction (qRT-PCR) was used to validate eight candidate circRNAs in 40 paired PTC tumors and adjacent normal samples. Next, we employed a bioinformatics tool to identify putative miRNA and circRNA-associated downstream genes, followed by constructing a network map of circRNA-miRNA-mRNA interactions and exploring the potential role of the candidate circRNAs. Results: In total, 206 up- and 177 downregulated circRNAs were identified in PTC tissues (fold change >1.5; P< 0.05). The expression levels of eight candidate circRNAs confirmed by qRT-PCR were significantly different between the PTC and normal samples. The downstream genes of candidate circRNAs participated in various biological processes and signaling pathways. The most up and downregulated circRNAs were hsa_circRNA_007148 and hsa_circRNA_047771. The lower expression level of hsa_circRNA_047771 was associated BRAFV600 mutation, lymph node metastasis (LNM), as well as with advanced TNM stage (all P<0.05). The higher expression level of hsa_circRNA_007148 was significantly correlated with LNM (P< 0.05). The areas under receiver operating curve were 0.876 (95% CI, 0.78-0.94) for hsa_circRNA_047771 and 0.846 (95% CI, 0.75-0.96) for hsa_circRNA_007148. Discussion: The study suggests that dysregulated circRNAs play a critical role in PTC pathogenesis. PTC-related hsa_circRNA_047771 and hsa_circRNA_007148 may serve as potential diagnostic biomarkers and prognostic predictors for PTC patients.

1   **Profile and Clinical Implication of Circular RNAs in Human Papillary Thyroid Carcinoma**

2   Huihui Ren[1#], Zhelong Liu[1#], Siyue Liu[1,] Xinrong Zhou[1], Hong Wang[2], Jinchao Xu[2], Daowen

3   Wang[1,2*], Gang Yuan[1*]

4   [1] Department of Internal Medicine, Tongji Hospital, Huazhong University of Science and

5   Technology, Wuhan, Hubei 430030, P.R. China

6   [2] Molecular Diagnostic Laboratory, Tongji Hospital, Huazhong University of Science and

7   Technology, Wuhan, Hubei 430030, P.R. China

8   [#]co-authors

9   [*]Corresponding author

10   Gang Yuan, MD, PhD, and Daowen Wang, MD, PhD

11   Department of Internal Medicine, Tongji Hospital, Tongji Medical College, Huazhong

12   University of Science & Technology, Wuhan 430030, China

13   Tel and Fax: +86-27-8366-2883

14   Email: gangyuan@tjh.tjmu.edu.cn and dwwang@tjh.tjmu.edu.cn

15   **Abstract**

16   **Background:** Differently expressed circular RNAs (circRNAs) have been reported to play a

17   considerable role in tumor behavior; however, the expression profile and biological function of

18   circRNAs in papillary thyroid carcinoma (PTC) remains unknown. Thus, the study was aimed to

19   characterize the circRNA expression profile to comprehensively understand the biological

20   behavior of PTC.

21   **Methods**: We investigated the expression profile of circRNAs using circRNA microarray in

22   three pairs of PTC and adjacent normal tissues. Quantitative real-time reverse transcription-

23   polymerase chain reaction (qRT-PCR) was used to validate eight candidate circRNAs in 40

24   paired PTC tumors and adjacent normal samples. Next, we employed a bioinformatics tool to

25   identify putative miRNA and circRNA-associated downstream genes, followed by constructing a

26   network map of circRNA-miRNA-mRNA interactions and exploring the potential role of the

27   candidate circRNAs.

28   **Results:** In total, 206 up- and 177 downregulated circRNAs were identified in PTC tissues (fold

29   change >1.5; P< 0.05). The expression levels of eight candidate circRNAs confirmed by qRT-

30   PCR were significantly different between the PTC and normal samples. The downstream genes

31   of candidate circRNAs participated in various biological processes and signaling pathways. The

32   most up and downregulated circRNAs were hsa_circRNA_007148 and hsa_circRNA_047771.

33   The lower expression level of hsa_circRNA_047771 was associated BRAFV600 mutation,

34   lymph node metastasis (LNM), as well as with advanced TNM stage (all P<0.05). The higher

35   expression level of hsa_circRNA_007148 was significantly correlated with LNM ($P < 0.05$). The

36   areas under receiver operating curve were 0.876 (95% CI, 0.78-0.94) for hsa_circRNA_047771

37   and 0.846 (95% CI, 0.75-0.96) for hsa_circRNA_007148.

38   **Discussion:** The study suggests that dysregulated circRNAs play a critical role in PTC

39   pathogenesis. PTC-related hsa_circRNA_047771 and hsa_circRNA_007148 may serve as

40   potential diagnostic biomarkers and prognostic predictors for PTC patients.

41 **Introduction**

42 Thyroid cancer is the most common malignant tumor of the endocrine organs, whose morbidity

43 has continuously increased in recent decades(La Vecchia et al. 2015; Siegel et al. 2017). The

44 dominant histological type is papillary thyroid carcinoma (PTC), which accounts for 85-95% of

45 all cases(La Vecchia et al. 2015). Although many studies have been performed to better

46 understand PTC, controversy remains regarding the malignancy diagnosis, postoperative

47 treatment, and prognosis in patients with thyroid nodules. Thyroid fine-needle aspiration biopsy

48 (FNAB) is a standard method for the preoperative evaluation of thyroid nodules, up to 30% of

49 nodules with indeterminate cytology; however, it cannot be definitively diagnosed(Haugen

50 2017). Operative treatment was suggested for most of these patients, although only 10-20% of

51 nodules were diagnosed as malignant lesions. An urgent clinical challenge is to develop an

52 effective diagnostic method to reduce overdiagnosis and overtreatment.

53 Recent studies have provided evidence that genetic factors may play a key role in the

54 development of thyroid cancer. The BRAFV600E mutation, resulting in activation of MAPK

55 pathway signaling, is significantly associated with more aggressive characteristics of PTCs and

56 is of great importance in risk-stratification and the management of patients with thyroid

57 nodules(Kwak et al. 2009; Xing 2007). In addition, various noncoding RNAs (ncRNAs), such as

58 microRNAs (miRNAs) and linear noncoding RNAs (lncRNAs), also participate in the

59 progression and pathogenesis of PTC(Fuziwara & Kimura 2016; Liyanarachchi et al. 2016).

60 However, the genomic and epigenomic mechanisms in thyroid cancer pathogenesis have not

61   been clarified.

62   Circular RNAs (circRNAs), a novel class of endogenous noncoding RNAs, have become a

63   research hotspot in the cancer field. Circular RNAs, unlike linear RNA, have no poly(A) tails

64   and 5′ caps, are characterized by a covalently closed loop structure formed by a tail 3′ splice site

65   and a head 5′ splice site(Jeck & Sharpless 2014). Recently, circRNAs were found to be highly

66   conserved in sequence, maintained stability in mammalian cells, and showed tissue-specific

67   expression(Chen & Schuman 2016; Rybak-Wolf et al. 2015). These properties make circRNAs

68   potential molecular biomarkers for multiple diseases. Furthermore, circRNAs are important

69   transcriptional regulators of gene expression involved in the pathogenesis of various diseases.

70   For example, circRNAs could function as miRNA sponges to compete with endogenous RNA,

71   regulating the expression of target genes(Zhao & Shen 2015). A human circRNA, ciRS-7

72   transcript (antisense to the cerebellar degeneration-related protein), acts as an miRNA-7 sponge

73   by binding to the microRNA effector complexes, which inactivate the function of miRNA(Lukiw

74   2013). Mounting evidence has demonstrated that circRNAs play a significant role in

75   carcinogenesis, acting as oncogenes or onco-suppressors. Differentially expressed circRNAs

76   were observed in various types of cancers and were associated with the development, invasion

77   and metastasis of human tumors(Chen et al. 2017; Han et al. 2017; Meng et al. 2017; Wu et al.

78   2010). These lines of evidence have suggested that circRNAs can be potential therapeutic targets

79   for diseases.

80   Although the association between circRNAs and various human cancers has been extensively

81 evaluated and well established, the diagnostic value and biological function of circRNAs in PTC

82 remain largely elusive. Until now, the only study focused on this issue was reported by Peng et

83 al.(Peng et al. 2017) and included 18 thyroid samples (six PTC, six paired contralateral normal

84 samples, and six benign thyroid lesions). Although a role of circRNAs in PTC pathogenesis was

85 observed, the clinical value of circRNAs for PTC diagnosis, therapy, and prognosis remains

86 undefined. The present study explored the circRNA expression profile in PTC and paired normal

87 tissues and examined the fundamental role of circRNAs in PTC, contributing not only to the

88 understanding of tumorigenesis but also to improving the diagnosis and management of thyroid

89 cancer.

90 **Materials and methods**

91 **Patients and tissue samples**

92 This study was approved by the Ethics Committee of Tongji Hospital, Tongji Medical, College,

93 Huazhong University of Science and Technology (RB approval number, TJ-C20150806).

94 Written consent was obtained from the patients before surgery. Forty PTC and matched adjacent

95 noncancerous tissue samples were obtained from patients who had undergone thyroidectomy at

96 the Department of General Surgery at Tongji Hospital Affiliated Huazhong University of

97 Science and Technology (Wuhan, Hubei province, China) from September 2016 to February

98 2017. All tissue samples were immediately soaked in RNAlater Reagent (Servicebio, Wuhan,

99 China) and were preserved at −80°C until further use. Of these samples, three pairs were used for

100 circRNA microarray analysis, and 40 samples (including the remaining 37 samples and the 3

101 samples used for microarray analysis) were used for additional validation in the present study.

102 The general clinicopathologic characteristics of the participants are shown in Table 1. None of

103 the participants included in this study underwent radiotherapy and chemotherapy preoperatively.

104 **Total RNA isolation and quality control**

105 Total RNA was isolated from PTC and paired adjacent normal tissues using a DNA/RNA

106 coextraction kit (Tiangen Biotech, Beijing, China; DP121221) according to the manufacturer′s

107 protocol. The purity and concentration of the total RNA samples were qualified and quantified

108 using the NanoDrop ND1000 system (NanoDrop Technologies/Thermo Scientific, Wilmington,

109 DE, USA). For spectrophotometry, the O.D. A260/A280 ratio should be close to 2.0 for pure

110 RNA. The O.D. A260/A230 ratio should be more than 1.8. The RNA integrity was assessed by

111 electrophoresis using a denaturing agarose gel.

Microarray analysis

113 The microarray analysis of circRNAs was performed based on the Arraystar's standard protocols

114 (Arraystar, Rockville, MD). Briefly, total RNA was digested with RNase R (Epicentre, Inc.) to

115 remove linear RNAs and enrich circular RNAs. Next, the enriched circular RNAs were amplified

116 and transcribed into fluorescent cRNA utilizing a random priming method (Arraystar Super RNA

117 Labeling Kit; Arraystar). The labeled cRNAs were hybridized onto the Arraystar Human

118 circRNA Array V2 (8×15K; Arraystar). After washing the slides, the arrays were scanned using

119 the Agilent Scanner G2505C system (Agilent, Santa Clara, CA).

Microarray data analysis

121 Agilent Feature Extraction software (version 11.0.1.1) was used to analyze acquired array

122 images. Quantile normalization and subsequent data processing were performed using the R

123 software limma package. Differentially expressed circRNAs with statistical significance between

124 two groups were identified through volcano plot filtering or fold change filtering. Hierarchical

125 clustering was performed to show the distinguishable circRNA expression patterns among the

126 samples. The interaction of circRNAs and miRNAs was predicted using Arraystar's homemade

127 miRNA target prediction software based on TargetScan and miRanda. All the differentially

128 expressed circRNAs were annotated in detail using the circRNA/miRNA interaction information.

Functional analysis

130   To further estimate the biological function of these candidate circRNAs, the targeted genes of

131   miRNAs that were predicted to interact with circRNAs were determined using TargetScan

132   (Enright et al. 2003) and miRanda (Pasquinelli et al. 2012). All miRNA gene targets were

133   identified by a p-value cutoff at 0.05. These putative target genes were then checked for

134   functional enrichment using DAVID (Database for Annotation, Visualization and Integrated

135   Discovery) (Huang da et al. 2009), and KEGG (Kyoto Encyclopedia of Genes and Genomes)

136   analysis was used to identify the significant pathways involved. The circRNA-miRNA-mRNA

137   interaction network was constructed by Cytoscape (http://www.cytoscape.org/) (Shang et al.

138   2016).

139   **Reverse transcription and qPCR validation**

140   For circRNA analysis, total RNA was reverse transcribed using the FastQuant RT kit (Tangent

141   Biotech, Beijing, China, KR106) and random primers. qRT-PCR was achieved using the Fast

142   SYBR® Green Master Mix (Thermo Fisher Scientific (Waltham, MA, USA) in a StepOne

143   Plus™ Real-Time PCR System (Applied Biosystems) with a 20-μL PCR reaction mixture that

144   included 2 μL of cDNA, 10 μL of Fast SYBRGreen Master Mix (2×), 0.2 μL of forward primer

145   (10 μM), 0.2 μL of reverse primer (10 μM), and 7.6 μL of nucleus-free water. The reactions

146   were incubated in a MicroAmp™ Fast Optical 96-well reaction plate at 95 ℃ for 20 sec,

147   followed by 40 cycles at 95 ℃ for 5 sec and 60 ℃ for 34 sec. The melting curve with a single

148   peak indicated the specific amplification of the expected fragments. The relative RNA

149   expression level was calculated using the ΔCt method. Divergent primers rather than the

150   commonly used convergent primers were designed for circular RNA amplification. The

151   sequences of GAPDH and circRNAs primers are listed in Supplementary Table S1. All

152   experiments were repeated three times.

153   **BRAFV600E mutation**

154   The BRAFV600E mutation was detected in the tumor tissues of these 40 PTC patients using

155   allelic-specific primer PCR (ASP-PCR). A 201-bp fragment was amplified using a primer

156   sequence designed for BRAF (Supplementary Table S1). The expected PCR products were

157   separated on agarose gels and visualized by golden view staining, followed by Sanger

158   sequencing validation.

159   **Statistical analysis**

160   All statistical data were analyzed using Statistical Product and Service Solutions SPSS software

161   19.0 (SPSS, Chicago, IL) and GraphPad Prism 5.0 (GraphPad Software, La Jolla, CA). The

162   differences in expression of circRNAs between PTC and paired adjacent normal tissues were

163   evaluated using Student's t test. The mean circRNA expression level was used as the cutoff value

164   to define the high and low expression of circRNAs. The correlations between the circRNA levels

165   and clinicopathological factors were analyzed by Student's t-test, Fisher's exact test, or

166   nonparametric test. A receiver operating curve (ROC) was established to assess the diagnostic

167   performance of hsa_circRNA_047771 and hsa_circRNA_007148. A P value <0.05 was

168   considered significant.

169   **Results**

170   **circRNA profiles in normal and tumor tissues**

171   To profile circRNA expression in PTC, we performed circRNA microarray analysis in PTC and

172   matched noncancerous thyroid tissues. Hierarchical clustering analysis indicated that the

173   expression patterns of circRNAs in PTC tissues were significantly different from those in normal

174   tissues (Fig. 1A, fold change > 1.5, p < 0.05). Red and green colors indicate the high and low

175   expression levels of circRNAs, respectively. The red point of the volcano plot determined the

176   significantly differentially expressed circRNAs between the normal and PTC samples with a fold

177   change>1.5 (Fig. 1B). The scatter plot revealed the difference in circRNA expression in PTC

178   tumor tissues and paired normal tissues (Fig. 1C). The points above and below the green lines

179   represent 1.5-fold up and down of circRNAs between the normal and PTC samples, respectively.

180   We found that 383 circRNAs were differentially expressed in PTC tissues compared with normal

181   tissues. Among them, 206 circRNAs were up regulated and 177 circRNAs were downregulated

182   (fold change ≥1.5, P< 0.05 and FDR < 0.05) in three paired carcinoma and normal tissues. The

183   differently deregulated circRNAs were mostly located in exons (Fig. 1D). The top 10

184   differentially expressed circRNAs are listed in Table 2.

185   **Validation of dysregulated circRNAs**

186   According to the fold change tested in the microarray analysis, eight circRNAs (four upregulated

187   and four downregulated) were selected for validation of the microarray results in 40 paired

188   nontumorous and tumor samples by qRT-PCR. All four upregulated and four downregulated

189 circRNAs were differentially expressed in PTC compared with those in normal tissues (Fig. 2A-

190 H). These results were consistent with the microarray data, indicating the validation of these

191 results.

192 **Functional analysis of differentially expressed circRNAs**

193 It is widely accepted that circRNAs are important transcriptional regulators of gene expression

194 involved in the pathogenesis of various cancers. To explore the underlying mechanisms of

195 dysregulated circRNAs involved in the tumorigenesis or development of PTC, Gene Ontology

196 (GO) enrichment analysis of differentially expressed target genes was performed to evaluate the

197 functional significance of these candidate circRNAs. The predominantly enriched GO items of

198 upregulated circRNAs in PTC were correlated with cell communication-related genes (Fig. 3A),

199 while the GO terms of downregulated circRNAs were mainly involved in the plasma membrane

200 (Fig. 3B). These enriched terms, involving cell communication, signal transducer activity, RNA

201 polymerase II transcription factor, and transcriptional activator activity, suggest that these

202 circRNAs play important roles in cell-to-cell signaling and interaction, cellular proliferation,

203 cellular function and maintenance.

204 KEGG analysis revealed that 50 pathways were significantly enriched among the target genes of

205 upregulated circRNAs (Bonferroni < 0.05), whereas 50 pathways were associated with

206 downregulated circRNAs (Bonferroni < 0.05). Notably, several important pathways were

207 enriched, such as the VEGF signaling pathway, ras signaling pathway, and Notch signaling

208 pathway (Fig. 4A, 4B). These findings suggest that circRNAs might play a significant role in

209   PTC carcinogenesis and metastasis.

210   **Clinical implications of novel circRNAs in PTC**

211   Based on the validation data, hsa_circRNA_007148 and hsa_circRNA_047771 were the most

212   significantly elevated and decreased in PTC samples compared with those in normal samples.

213   Therefore, we evaluated their potential clinical value by analyzing the correlation of these two

214   candidate circRNAs with several clinicopathological parameters of PTC patients. Table 3 shows

215   that lower hsa_circRNA_047771 expression levels were associated with BRAFV600 mutation,

216   lymph node metastasis (LNM), and TNM stage (all P<0.05). However, we observed no

217   association between the hsa_circRNA_047771 expression levels and other clinicopathological

218   factors, including sex, age, a history of Hashimoto's thyroiditis, thyroid imaging reporting and

219   data system (TIRAIDS), tumor size, and multifocality. We further found that a higher expression

220   level of hsa_circRNA_007148 was significantly correlated with LNM (P< 0.05), while no other

221   clinicopathological factor was found to be significantly associated with the

222   hsa_circRNA_007148 expression level (P>0.05). Additionally, similar associations were found

223   with the other six deregulated circRNAs (Supplementary Table S2). Next, we performed ROC

224   curve analysis to assess the diagnostic value of hsa_circRNA_047771 and hsa_circRNA_007148

225   in distinguishing PTC tissues from normal tissues. The areas under ROC curve were 0.876 (95%

226   CI, 0.78-0.94) for hsa_circRNA_047771 and 0.846 (95% CI, 0.75-0.96) for

227   hsa_circRNA_007148 (Fig. 5A, 5B; Table 4).

228   **Bioinformatics analysis of hsa_circRNA_047771 and hsa_circRNA_007148**

229   We next used Arraystar's circRNA target prediction software to identify potential miRNAs that

230   could bind to hsa_circRNA_047771 and hsa_circRNA_007148 via miRNA response elements

231   (MREs). The top 5 ranking MRE targets for the differentially expressed circRNAs are shown in

232   supplementary Figs. S1, 2. Notably, among the list of miRNAs targeted by

233   hsa_circRNA_047771, miR-522-3p/miR-153-5p were implicated in PTC in previous reports. We

234   further detected the expression levels of miR-522-3p/miR-153-5p in the 40 paired PTC and

235   normal samples. miR-522-3p/miR-153-5p were upregulated in PTC tissues compared with those

236   in adjacent normal tissues (supplementary Fig. S3). These results provide powerful evidence that

237   hsa_circRNA_047771/ miR-522-3p/miR-153-5p could participate in the pathogenesis of PTC.

238   To fully understand the underlying mechanism between deregulated circRNAs and the biological

239   progress of PTC, the target prediction program was performed to predict the potential target

240   genes in the database. Based on the data of the deregulated circRNAs, their predicted MREs and

241   targeted genes, we constructed a network map of cancer related circRNA-miRNA-mRNA

242   interactions using Cytoscape that included 36 mRNAs and 34 miRNAs for

243   hsa_circRNA_047771 and 41 mRNAs and 51 miRNAs for hsa_circRNA_007148 (Fig. 6A, 6B).

244 **Discussion**

245 Recently, the crucial role of epigenetic regulation in the development and pathogenesis of

246 cancers has been widely recognized. There is abundant evidence suggesting that ncRNAs,

247 including miRNAs, lncRNAs and circular RNAs, are strongly associated with the biological

248 behavior of tumors. However, the role of circRNAs in PTC remains largely unknown. In the

249 present study, we characterized the expression profile of circRNAs in PTC tissues and identified

250 many aberrantly expressed circRNAs in PTC tissues, followed by validation of eight

251 significantly different expressed circRNAs. Bioinformatics analysis indicated that deregulated

252 circRNAs might be implicated in the biological process of PTC by regulating tumor-related

253 pathways. The association between two novel circRNAs and aggressive clinicopathological

254 characteristics provide evidence that circRNAs may serve as prognostic predictors for PTC

255 patients. Additionally, the areas under ROC curve suggest that hsa_circRNA_047771 and

256 hsa_circRNA_007148 may be candidate diagnostic biomarkers for PTC.

257 PTC accounts for a large proportion of thyroid cancer and needs to be better characterized and

258 understood. Although the functions of circRNAs in carcinogenesis and cancer development have

259 drawn great attention, studies focused on the role of circRNAs in PTC remain scarce. To our

260 knowledge, only one study has focused on the relationship between circRNAs and PTC(Peng et

261 al. 2017). This study performed circRNA microarray on 6 paired PTC tumors and contralateral

262 normal tissues, as well as six benign thyroid nodules, to investigate the profile of circRNA

263 expression in PTC and identified one significantly downregulated circRNA

264   (hsa_circRNA_100395) that was associated with two tumor-associated miRNA clusters (miR-

265   141-3p and miR-200a-3p), revealing a potential role of circRNAs in PTC pathogenesis.

266   However, to date, no study has investigated the clinical value of circRNAs in PTC patients. The

267   association between circRNA expression and prognosis factors of PTC, such as tumor size,

268   tumor stage, LNM, and BRAF mutation, remains unclear. It is crucial to understand the

269   underlying mechanism of circRNAs regarding tumor behavior at the molecular level with a

270   larger sample. It will be of great importance to identify novel diagnostic, prognostic, and

271   therapeutic targets. Thus, we performed circular RNA array to characterize the circRNA

272   expression profile to comprehensively understand its clinical implications in PTC. Furthermore,

273   similar to Nianchun Peng et al.(Peng et al. 2017), our study identified deregulated circRNAs. In

274   the present study, KEGG and GO enrichment analyses identified many significant terms

275   involved in cell events and several important cancer-related signaling pathways, such as the

276   VEGF signaling pathway, ras signaling pathway, and Notch signaling pathway. Particularly, the

277   ras signaling pathway was implicated in the development of PTC. These findings suggest that

278   circRNAs might play a significant role in PTC carcinogenesis and metastasis.

279   Our study identified two novel circRNAs that were significantly associated with aggressive

280   prognostic features of PTC, such as LNM and advanced TNM stage. These data indicated that

281   deregulated circRNAs could predict the prognosis of patients with PTC. Interestingly, we found

282   that a lower expression of hsa_circRNA_047771 is more likely to manifest with BRAFV600E

283   mutation. BRAFV600E mutation has emerged as a poor prognostic marker for PTC patients. The

284   clinical usefulness of BRAFV600E in the risk stratification, diagnosis and management of PTC

285   patients has been established(Elisei et al. 2008; Lupi et al. 2007). The predictive effect of

286   circRNAs in the prognosis of PTC patients and its association with BRAFV600E mutation in

287   PTC patients are considerably important and need further investigation.

288   The clinical application of circRNAs as potential molecular markers for the diagnosis and

289   treatment of disease are promising(Meng et al. 2017), as confirmed by our results. circRNAs are

290   highly stable and conservative in the cytoplasm and other body fluids, such as saliva and

291   exosomes(Bahn et al. 2015; Dou et al. 2016). The observed high stability of circRNAs suggests

292   that circRNAs will likely be a reliable biomarker for the preoperative diagnosis of PTC. Given

293   the diagnostic limitations of FNAB in indeterminate cytology and insufficient sensitivity of

294   molecular testing(Haugen et al. 2016; Li et al. 2015), the detection of circRNAs and clinical

295   significance of circRNAs used for the preoperative diagnosis of thyroid cancers are attractive

296   and critical issues related to thyroid cancer study that need to be well defined.

297   Circular RNAs are endogenous ncRNA molecules that function as regulators involved in various

298   biological courses of cancer, such as development and proliferation(He et al. 2017; Xin et al.

299   2017). The mechanisms underlying circRNAs and tumorigenesis may be primarily associated

300   with altered gene expression mediated by acting as an miRNA sponge(Chen et al. 2015). Recent

301   studies have revealed that aberrant circRNA expression was closely correlated with various

302   cancers, including hepatocellular carcinoma, colon cancer, breast cancer, esophageal cancer, and

303   oral cancer(Chen et al. 2017; Han et al. 2017; Hsiao et al. 2017; Lu et al. 2017). Chen et al.(Chen

304 et al. 2017) found that circRNA_100290 could regulate oral squamous cell carcinomas through

305 miR-29b-mediated inhibition of cell proliferation and the reduction of CDK6 expression.

306 Another circRNA identified in a recent study, termed circHIPK3, was observed to be

307 differentially expressed in several normal and tumor tissues and functions as a gene regulator by

308 regulating miRNA activity(Zheng et al. 2016). These findings were confirmed in our study. We

309 observed that each circRNA could bind to multiple miRNAs, some of which have been reported

310 to be involved in PTC biology. For example, we found that miR-522-3p/miR-153-5p were

311 targets of one novel down-expressed circRNA (hsa_circRNA_047771). These deregulated

312 miRNAs have been reported to significantly correlate with thyroid cancer differentiation and

313 progression(Boufraqech et al. 2016; Fuziwara & Kimura 2016). Thus, further investigations are

314 necessary to clarify the specific mechanism between deregulated circRNAs and PTC pathology.

315 Several limitations of this study must be addressed. First, the sample size was limited, and other

316 thyroid carcinomas were not included in this study other than PTC. Second, we did not clarify

317 the mechanism of circRNA/miRNA in the PTC pathological process. The molecular mechanism

318 should be experimentally determined and elaborated in the future. Third, given the clinical

319 applications of circRNAs, further studies will be required to evaluate the diagnostic value of

320 circRNA levels in serum or FNAB samples.

321 **Conclusions**

322 The study demonstrated that several circRNAs are expressed differently in PTC and participate

323 in tumor pathogenesis. Two PTC-associated circRNAs could serve as potential diagnostic

324   markers and predict the prognosis of PTC patients. Furthermore, the study revealed that

325   circRNAs may have great potential as prognosis predictors and therapeutic targets for PTC

326   patients in the near future.

327 **References**

328 Bahn JH, Zhang Q, Li F, Chan TM, Lin X, Kim Y, Wong DT, and Xiao X. 2015. The landscape

329   of microRNA, Piwi-interacting RNA, and circular RNA in human saliva. *Clin Chem*

330   61:221-230. 10.1373/clinchem.2014.230433

331 Boufraqech M, Klubo-Gwiezdzinska J, and Kebebew E. 2016. MicroRNAs in the thyroid. *Best*

332   *Pract Res Clin Endocrinol Metab* 30:603-619. 10.1016/j.beem.2016.10.001

333 Chen I, Chen CY, and Chuang TJ. 2015. Biogenesis, identification, and function of exonic

334   circular RNAs. *Wiley Interdiscip Rev RNA* 6:563-579. 10.1002/wrna.1294

335 Chen L, Zhang S, Wu J, Cui J, Zhong L, Zeng L, and Ge S. 2017. circRNA_100290 plays a role

336   in oral cancer by functioning as a sponge of the miR-29 family. *Oncogene*.

337   10.1038/onc.2017.89

338 Chen W, and Schuman E. 2016. Circular RNAs in Brain and Other Tissues: A Functional

339   Enigma. *Trends Neurosci* 39:597-604. 10.1016/j.tins.2016.06.006

340 Dou Y, Cha DJ, Franklin JL, Higginbotham JN, Jeppesen DK, Weaver AM, Prasad N, Levy S,

341   Coffey RJ, Patton JG, and Zhang B. 2016. Circular RNAs are down-regulated in KRAS

342   mutant colon cancer cells and can be transferred to exosomes. *Sci Rep* 6:37982.

343   10.1038/srep37982

344 Elisei R, Ugolini C, Viola D, Lupi C, Biagini A, Giannini R, Romei C, Miccoli P, Pinchera A,

345   and Basolo F. 2008. BRAF(V600E) mutation and outcome of patients with papillary

346   thyroid carcinoma: a 15-year median follow-up study. *J Clin Endocrinol Metab* 93:3943-

347   3949. 10.1210/jc.2008-0607

348   Enright AJ, John B, Gaul U, Tuschl T, Sander C, Marks DS: MicroRNA targets in Drosophila.

349   Genome biology 2003; 5(1):R1.

350   Fuziwara CS, and Kimura ET. 2016. MicroRNAs in thyroid development, function and

351   tumorigenesis. *Mol Cell Endocrinol*. 10.1016/j.mce.2016.12.017

352   Han D, Li J, Wang H, Su X, Hou J, Gu Y, Qian C, Lin Y, Liu X, Huang M, Li N, Zhou W, Yu

353   Y, and Cao X. 2017. Circular RNA MTO1 acts as the sponge of miR-9 to suppress

354   hepatocellular carcinoma progression. *Hepatology*. 10.1002/hep.29270

355   Haugen BR. 2017. 2015 American Thyroid Association Management Guidelines for Adult

356   Patients with Thyroid Nodules and Differentiated Thyroid Cancer: What is new and what

357   has changed? *Cancer* 123:372-381. 10.1002/cncr.30360

358   Haugen BR, Alexander EK, Bible KC, Doherty GM, Mandel SJ, Nikiforov YE, Pacini F,

359   Randolph GW, Sawka AM, Schlumberger M, Schuff KG, Sherman SI, Sosa JA, Steward

360   DL, Tuttle RM, and Wartofsky L. 2016. 2015 American Thyroid Association

361   Management Guidelines for Adult Patients with Thyroid Nodules and Differentiated

362   Thyroid Cancer: The American Thyroid Association Guidelines Task Force on Thyroid

363   Nodules and Differentiated Thyroid Cancer. *Thyroid* 26:1-133. 10.1089/thy.2015.0020

364   He J, Xie Q, Xu H, Li J, and Li Y. 2017. Circular RNAs and cancer. *Cancer Lett* 396:138-144.

365   10.1016/j.canlet.2017.03.027

366   Hsiao KY, Lin YC, Gupta SK, Chang N, Yen L, Sun HS, and Tsai SJ. 2017. Noncoding Effects

367   of Circular RNA CCDC66 Promote Colon Cancer Growth and Metastasis. *Cancer Res*

368   77:2339-2350. 10.1158/0008-5472.can-16-1883

369   Huang da W, Sherman BT, Lempicki RA: Systematic and integrative analysis of large gene lists

370   using DAVID bioinformatics resources. Nature protocols 2009; 4(1):44-57.

371   Jeck WR, and Sharpless NE. 2014. Detecting and characterizing circular RNAs. *Nat Biotechnol*

372   32:453-461. 10.1038/nbt.2890

373   Kwak JY, Kim EK, Chung WY, Moon HJ, Kim MJ, and Choi JR. 2009. Association of

374   BRAFV600E mutation with poor clinical prognostic factors and US features in Korean

375   patients with papillary thyroid microcarcinoma. *Radiology* 253:854-860.

376   10.1148/radiol.2533090471

377   La Vecchia C, Malvezzi M, Bosetti C, Garavello W, Bertuccio P, Levi F, and Negri E. 2015.

378   Thyroid cancer mortality and incidence: a global overview. *Int J Cancer* 136:2187-2195.

379   10.1002/ijc.29251

380   Li F, Chen G, Sheng C, Gusdon AM, Huang Y, Lv Z, Xu H, Xing M, and Qu S. 2015.

381   BRAFV600E mutation in papillary thyroid microcarcinoma: a meta-analysis. *Endocr*

382   *Relat Cancer* 22:159-168. 10.1530/erc-14-0531

383   Liyanarachchi S, Li W, Yan P, Bundschuh R, Brock P, Senter L, Ringel MD, de la Chapelle A,

384   and He H. 2016. Genome-Wide Expression Screening Discloses Long Noncoding RNAs

385   Involved in Thyroid Carcinogenesis. *J Clin Endocrinol Metab* 101:4005-4013.

386   10.1210/jc.2016-1991

387   Lu L, Sun J, Shi P, Kong W, Xu K, He B, Zhang S, and Wang J. 2017. Identification of circular

388   RNAs as a promising new class of diagnostic biomarkers for human breast cancer.

389   *Oncotarget*. 10.18632/oncotarget.17307

390   Lukiw WJ. 2013. Circular RNA (circRNA) in Alzheimer's disease (AD). *Front Genet* 4:307.

391   10.3389/fgene.2013.00307

392   Lupi C, Giannini R, Ugolini C, Proietti A, Berti P, Minuto M, Materazzi G, Elisei R, Santoro M,

393   Miccoli P, and Basolo F. 2007. Association of BRAF V600E mutation with poor

394   clinicopathological outcomes in 500 consecutive cases of papillary thyroid carcinoma. *J

395   Clin Endocrinol Metab* 92:4085-4090. 10.1210/jc.2007-1179

396   Meng S, Zhou H, Feng Z, Xu Z, Tang Y, Li P, and Wu M. 2017. CircRNA: functions and

397   properties of a novel potential biomarker for cancer. *Mol Cancer* 16:94. 10.1186/s12943-

398   017-0663-2

399   Pasquinelli AE: MicroRNAs and their targets: recognition, regulation and an emerging reciprocal

400   relationship. Nature reviews Genetics 2012; 13(4):271-282.

401   Peng N, Shi L, Zhang Q, Hu Y, Wang N, and Ye H. 2017. Microarray profiling of circular RNAs

402   in human papillary thyroid carcinoma. *PLoS One* 12:e0170287.

403   10.1371/journal.pone.0170287

404   Rybak-Wolf A, Stottmeister C, Glazar P, Jens M, Pino N, Giusti S, Hanan M, Behm M, Bartok

405   O, Ashwal-Fluss R, Herzog M, Schreyer L, Papavasileiou P, Ivanov A, Ohman M,

406   Refojo D, Kadener S, and Rajewsky N. 2015. Circular RNAs in the Mammalian Brain

407   Are Highly Abundant, Conserved, and Dynamically Expressed. *Mol Cell* 58:870-885.

408   10.1016/j.molcel.2015.03.027

409   Shang X, Li G, Liu H, Li T, Liu J, Zhao Q, Wang C: Comprehensive Circular RNA Profiling

410   Reveals That hsa_circ_0005075, a New Circular RNA Biomarker, Is Involved in

411   Hepatocellular Crcinoma Development. Medicine 2016; 95(22):e3811.

412   Siegel RL, Miller KD, and Jemal A. 2017. Cancer Statistics, 2017. *CA Cancer J Clin* 67:7-30.

413   10.3322/caac.21387

414   Wu ZS, Wu Q, Wang CQ, Wang XN, Wang Y, Zhao JJ, Mao SS, Zhang GH, Zhang N, and Xu

415   XC. 2010. MiR-339-5p inhibits breast cancer cell migration and invasion in vitro and

416   may be a potential biomarker for breast cancer prognosis. *BMC Cancer* 10:542.

417   10.1186/1471-2407-10-542

418   Xin Z, Ma Q, Ren S, Wang G, and Li F. 2017. The understanding of circular RNAs as special

419   triggers in carcinogenesis. *Brief Funct Genomics* 16:80-86. 10.1093/bfgp/elw001

420   Xing M. 2007. BRAF mutation in papillary thyroid cancer: pathogenic role, molecular bases, and

421   clinical implications. *Endocr Rev* 28:742-762. 10.1210/er.2007-0007

422   Zhao ZJ, and Shen J. 2015. Circular RNA participates in the carcinogenesis and the malignant

423   behavior of cancer. *RNA Biol*:1-8. 10.1080/15476286.2015.1122162

424   Zheng Q, Bao C, Guo W, Li S, Chen J, Chen B, Luo Y, Lyu D, Li Y, Shi G, Liang L, Gu J, He

425   X, and Huang S. 2016. Circular RNA profiling reveals an abundant circHIPK3 that

426   regulates cell growth by sponging multiple miRNAs. *Nat Commun* 7:11215.

427   10.1038/ncomms11215

428   **Figure legends**

429   **Fig. 1. circRNA expression profile in papillary thyroid carcinoma and paired normal**

430   **tissues.** (A) Heat map from the microarray analysis of circRNA expression in normal and

431   papillary thyroid carcinoma (PTC) tissues (fold change > 1.5, p < 0.05). Red and green colors

432   indicate high and low expression levels, respectively. (B) Volcano plot constructed to visualize

433   the differentially expressed circRNAs between PTC and adjacent normal tissues. The vertical

434   lines indicate 1.5-fold upregulation and downregulation. The horizontal line represents a P-value

435   of 0.05. The red points in the plot represent the statistically deregulated circRNAs. (C) Scatter

436   plots represent the differential expression of circRNAs in PTC tumors (group-C) versus normal

437   thyroid tissue (group-N). The values of the x- and y-axes in the scatter plot were the normalized

438   signal intensities of the samples (log2 scaled). The green lines represent the 1.5-fold up and

439   down of circRNAs between the normal and PTC samples. C: PTC tissue. N: adjacent normal

440   tissue. (D) the proportion of differentially expressed circRNAs according to the different

441   genomic locus (exonic, intronic, antisense, intragenic, and intergenic).

442   **Fig. 2. Identification and qRT-PCR validation of differentially expressed circRNAs.** (A-D),

443   (E-H) The relative expression of four upregulated and four downregulated circRNAs was

444   validated in 40 human PTC tissues and adjacent non-tumorous tissues. ***P<0.001. Normal:

445   adjacent non-tumorous tissue; PTC: papillary thyroid tumor tissue. ΔCt values were used to

446   assess the relative gene expression, which was normalized to the GAPDH expression level.

447   **Fig. 3. Enrichment GO analysis of circRNA-target genes.** Top 10 significant enriched GO

448   terms of upregulated circRNAs(A) and downregulated circRNAs (B).

449   **Fig. 4. Enrichment KEGG analysis of circRNA-target genes.** Top 10 pathway terms in KEGG

450   pathway analysis of upregulated circRNAs (A) and downregulated circRNAs (B).

451   **Fig. 5. Correlation of hsa_circRNA_047771 and hsa_circRNA_007148 with the diagnosis of**

452   **papillary thyroid carcinoma patients.** Receiver operating characteristics (ROC) curve analysis

453   for hsa_circRNA_047771(A) and hsa_circRNA_007148) (B) according to their relative

454   expression level as measured by qPCR ($P<0.01$).

455   **Fig. 6. Construction of the circRNA-miRNA-mRNA network**. (A) The network map

456   contained the significantly upregulated hsa_circRNA_007148 (represented by brown nodes)

457   along with their 51 downstream miRNAs (represented by red nodes) and 41 target mRNAs

458   (represented by light-blue nodes). (B) The network map contained significantly downregulated

459   hsa_circRNA_047771 (represented by brown nodes) along with their 34 downstream miRNAs

460   (represented by red nodes) and target 36 mRNAs (represented by light-blue nodes).

Figure 1

circRNAs expression profile in papillary thyroid carcinoma and paired normal tissues.

(A) Heat map from the microarray analysis of circRNA expression in normal and p apillary thyroid carcinoma (PTC) tissues (fold change > 1.5, p < 0.05). Red and green colors indicate high and low expression levels, respectively. (B) Scatter plots represent the differential expression of circRNAs in PTC tumors (group-C) versus normal thyroid tissue (group-N). The values of the x- and y-axes in the scatter plot were the normalized signal intensities of the samples (log2 scaled). The green lines represent the 1.5-fold up and down of circRNAs between the normal and PTC samples. C: PTC tissue. N: adjacent normal tissue. (C) Volcano plot constructed to visualize the differentially expressed circRNAs between PTC and adjacent normal tissues. The vertical lines indicate 1.5-fold upregulation and downregulation. The horizontal line represents a *P*-value of 0.05. The red points in the plot represent the statistically deregulated circRNAs. (D) the proportion of differentially expressed circRNAs according to the different genomic locus (exonic, intronic, antisense, intragenic, and intergenic).
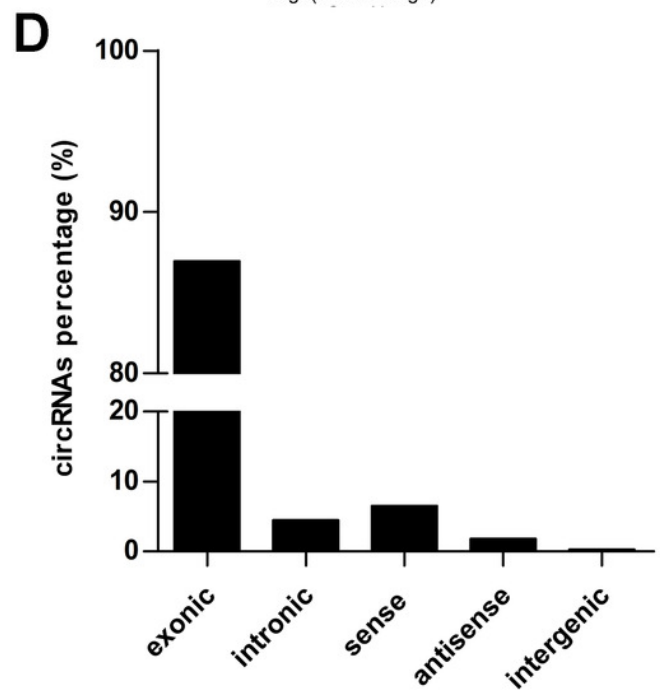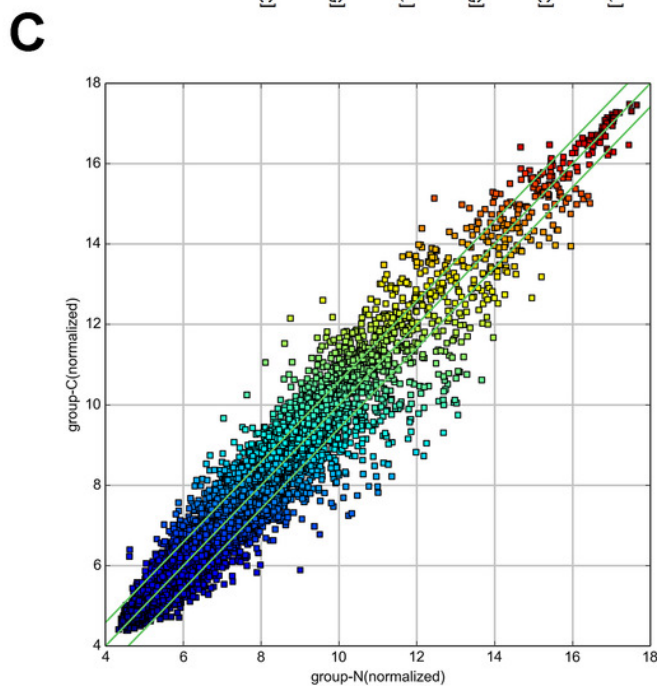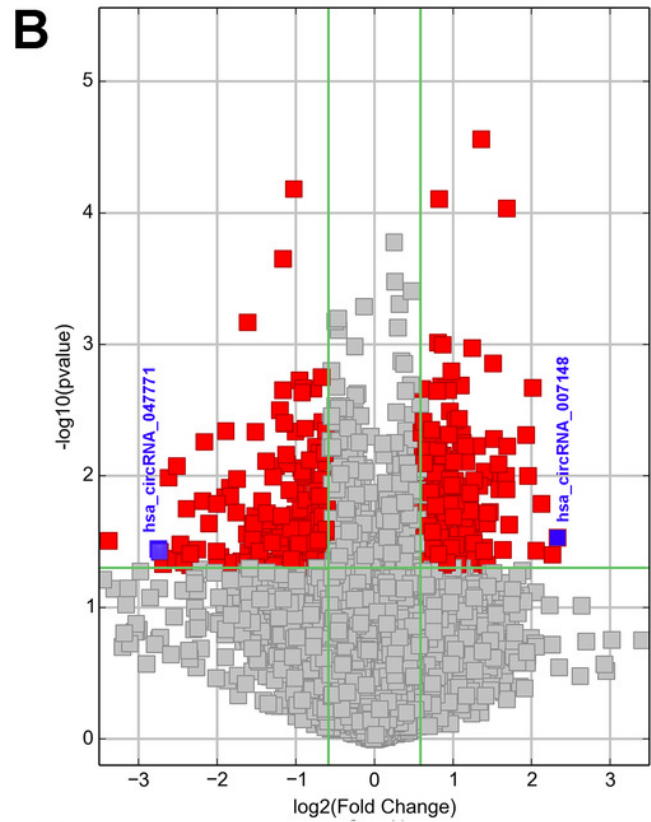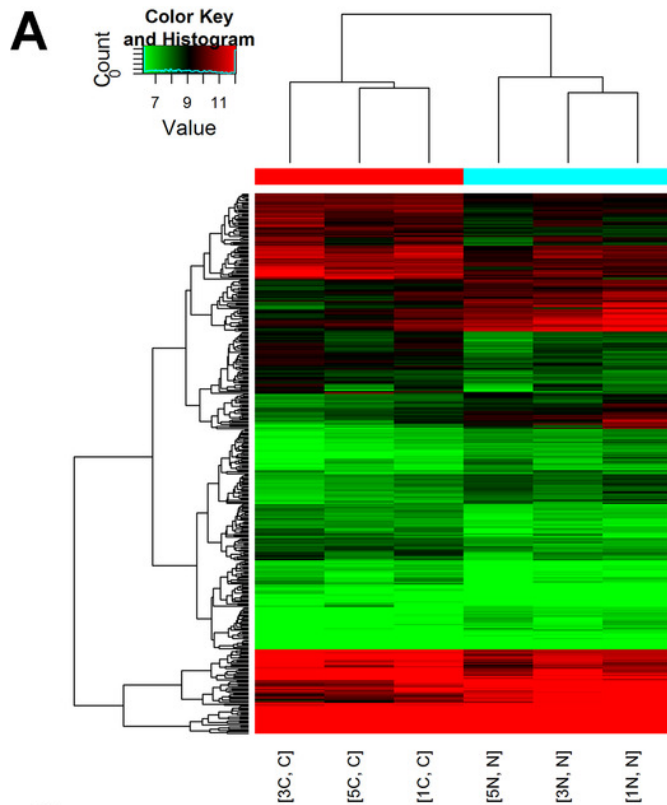
Figure 2

Identification and qRT-PCR validation of differentially expressed circRNAs.

(A-D), (E-H) The relative expression of four upregulated and four downregulated circRNAs was validated in 40 human PTC tissues and adjacent non-tumorous tissues. *** P <0.001. Normal: adjacent non-tumorous tissue; PTC: papillary thyroid tumor tissue. ΔCt values were used to assess the relative gene expression, which was normalized to the GAPDH expression level.
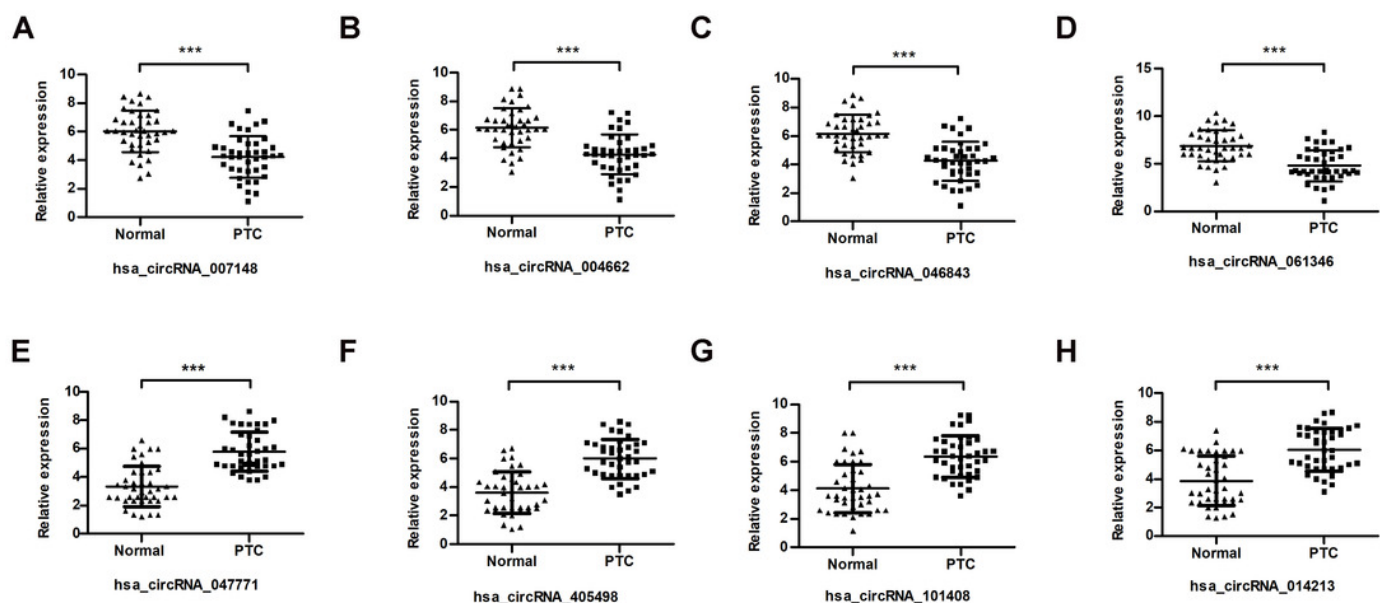
Figure 3

Enrichment analysis of circRNA-target genes.

Top 10 significant enriched GO terms of upregulated circRNAs(A) and downregulated circRNAs (B).

A
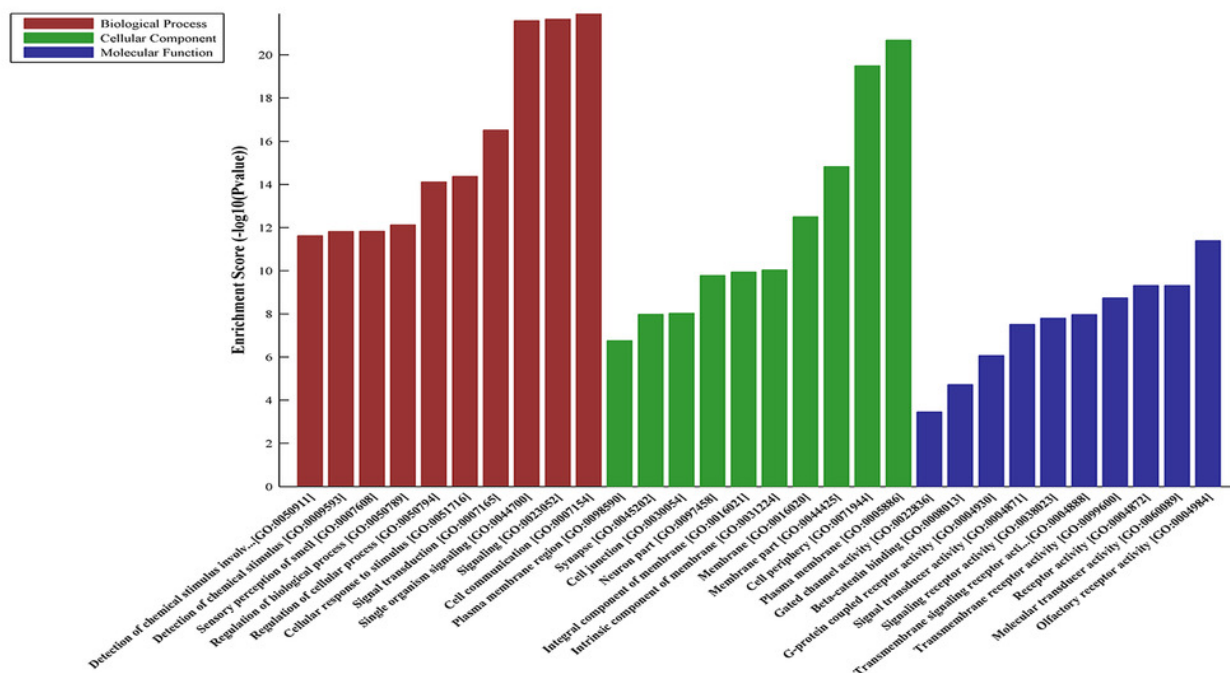
B
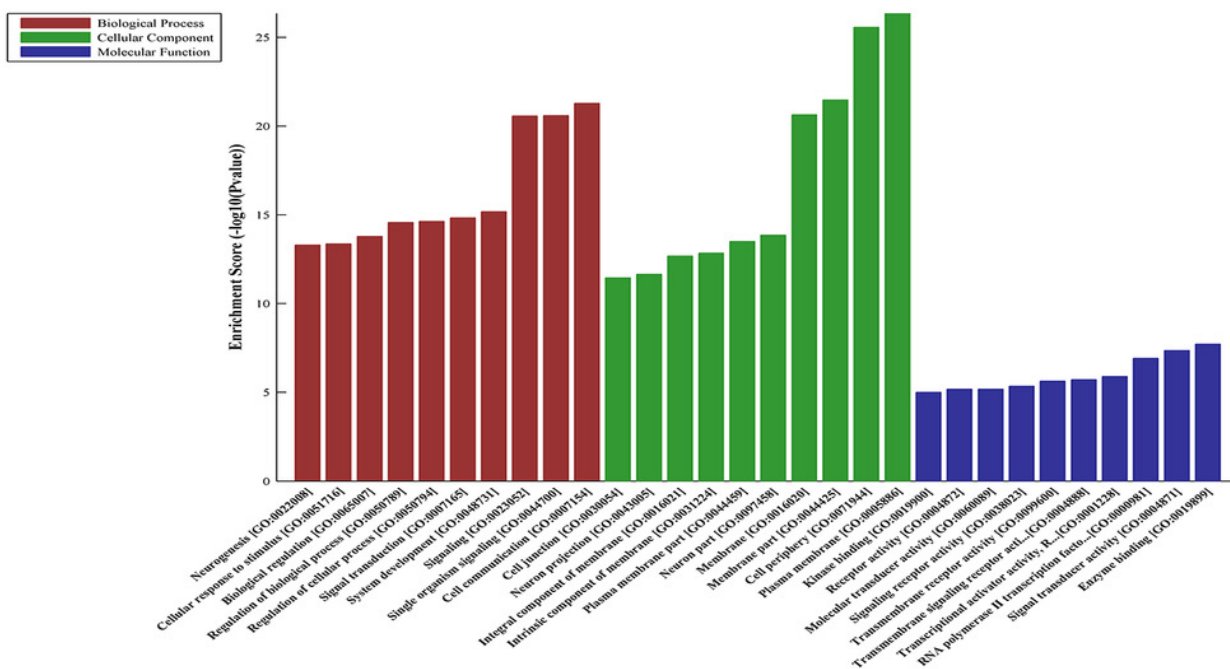
Figure 4

Enrichment KEGG analysis of circRNA-target genes.

Top 10 pathway terms in KEGG pathway analysis of upregulated circRNAs (A) and downregulated circRNAs (B).
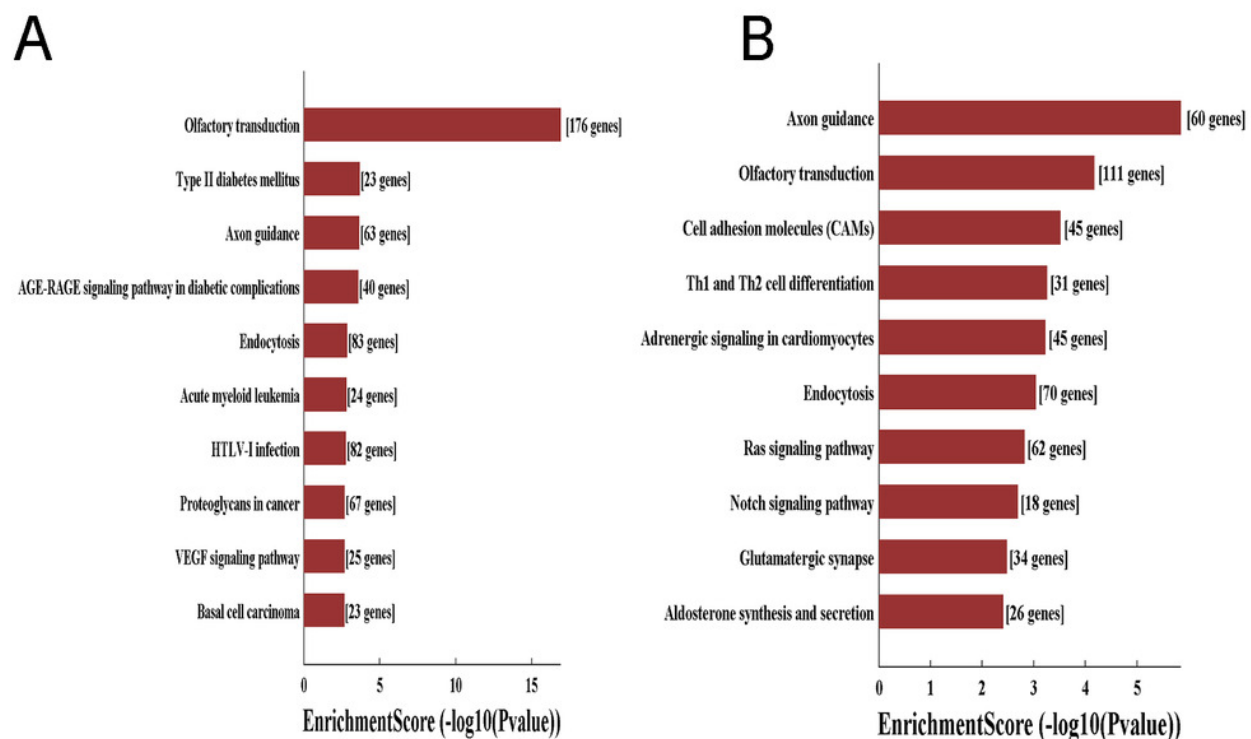
Figure 5

Correlation of hsa_circRNA_047771 and hsa_circRNA_007148 with the diagnosisof papillary thyroid carcinoma patients.

Receiver operating characteristics (ROC) curve analysis for hsa_circRNA_047771(A) and hsa_circRNA_007148) (B) according to their relative expression level as measured by qPCR (*P*<0.01).
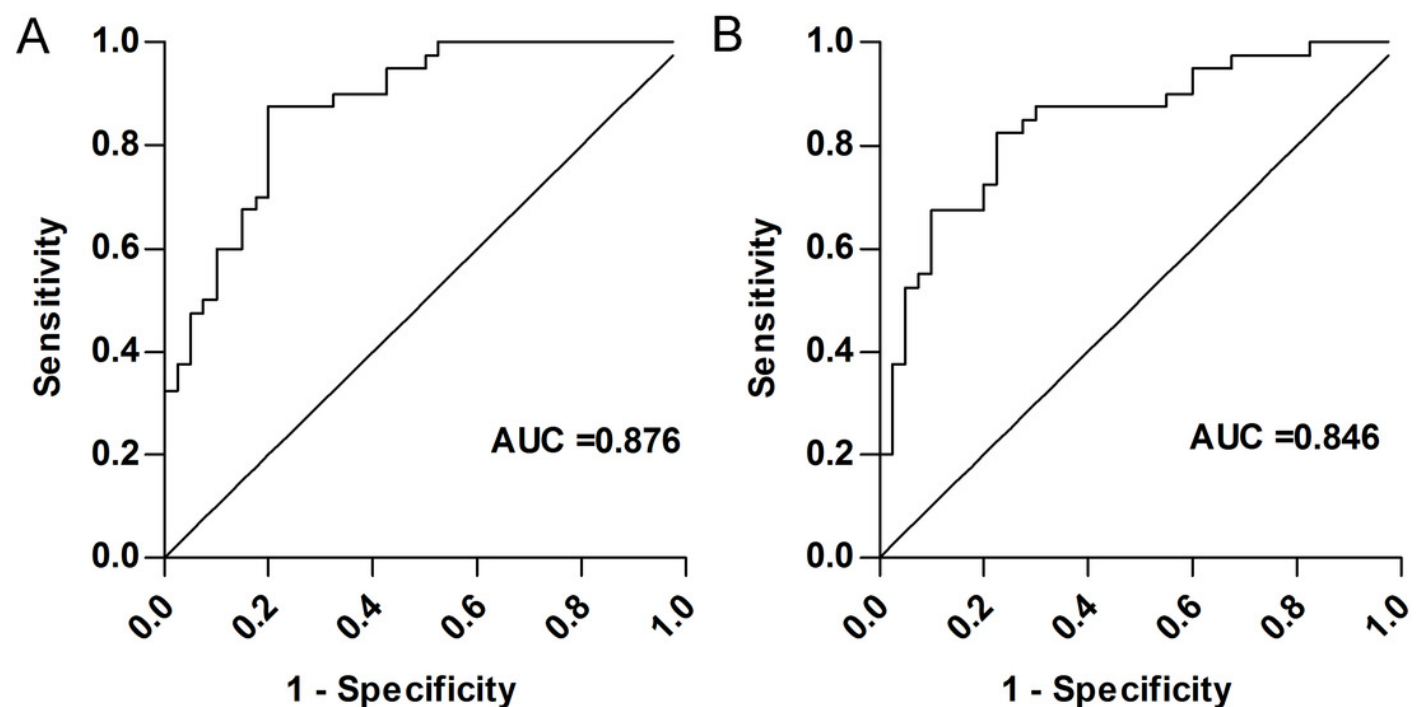
Figure 6

Construction of the circRNA-miRNA-mRNAnetwork .

(A) The network map contained the significantly upregulated hsa_circRNA_007148 (represented by brown nodes) along with their 51 downstream miRNAs (represented by red nodes) and 41 target mRNAs (represented by light-blue nodes). (B) The network map contained significantly downregulated hsa_circRNA_047771 (represented by brown nodes) along with their 34 downstream miRNAs (represented by red nodes) and target 36 mRNAs (represented by light-blue nodes).
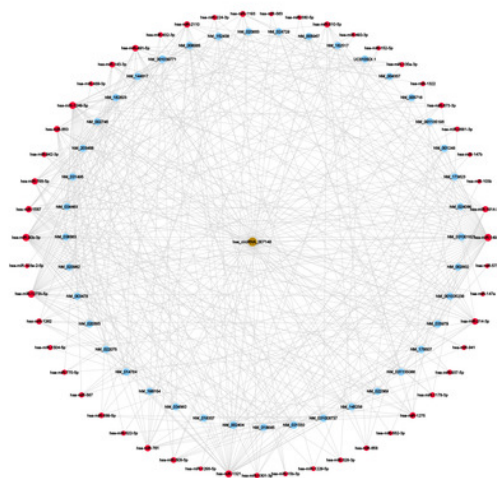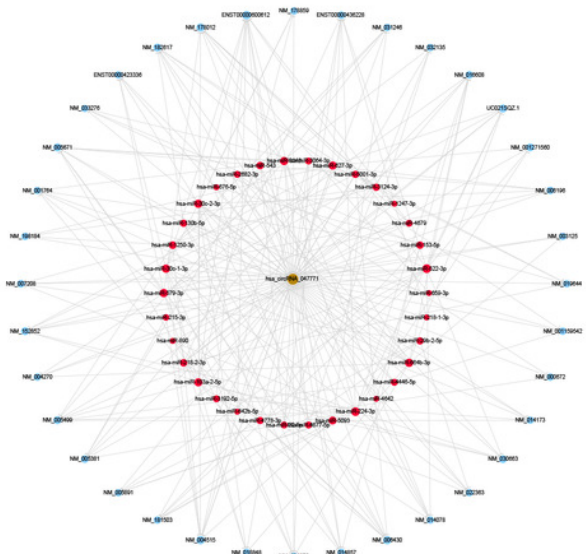
Clinicopathological characteristics of participating patients.

Data are expressed as mean (sd) or n(percent) or median (interquartile range); TIRAIDS, thyroid imaging reporting and data system; TNM, tumor-node-metastasis. LNM, lymph node metastasis.

1   Table 1. Clinicopathological characteristics of participates patients.

	Patients(n=40)
Age(years)	43.5(13.1)
≥45	21(52.5)
<45	19(47.5)
Sex	
Female	30(75)
male	10(25)
Hashimoto	
Yes	6(15)
No	34(85)
TIRAID	
4a	4(10)
4b	13(32.5)
4c	23(57.5)
BRAF mutation	
Yes	16(40)
No	24(60)
Tumor size (cm)	1.2(0.8-2)
TNM stage	
I	25(62.59)
II	0
III	9(22.5)
IV	6(15)
LNM	
Yes	18(45)
No	22(55)
Focality	
Unifocal	13(32.5)
Multifocal	27(67.5)

2   Data are expressed as mean (sd) or n(percent) or median (interquartile

3   range); TIRAIDS, thyroid imaging reporting and data system; TNM,

4   tumor-node-metastasis. LNM, lymph node metastasis

Top 10 most upregulated and downregulated circRNAs in PTC tumors versus paired normal thyroid tissue.

1 Table 2. Top 10 most upregulated and downregulated circRNAs in PTC tumors versus paired normal thyroid tissue.

circRNA	FC	P value	Type	chrom	GeneSymbol	miRNA binding sites
upregulated						
hsa_circRNA_007148	5.014	0.02933	exonic	chr3	FNDC3B	hsa-miR-6785-5p,hsa-miR-1275,hsa-miR-490-3p,hsa-miR-1229-5p,hsa-miR-6088
hsa_circRNA_004662	4.80	0.03966	exonic	chr6	SOD2	hsa-miR-4520-2-3p,hsa-miR-208b-5p,hsa-miR-4713-5p,hsa-miR-4659b-3p
hsa_circRNA_046843	4.36	0.01622	exonic	chr18	ANKRD12	hsa-miR-4524a-5p,hsa-miR-4753-3p,hsa-miR-3911,hsa-miR-876-5p,hsa-miR-942-5p
hsa_circRNA_103514	4.16	0.03694	exonic	chr3	FNDC3B	hsa-miR-147b,hsa-miR-510-5p,hsa-miR-15b-3p,hsa-miR-1323,hsa-miR-552-3p
hsa_circRNA_061346	4.03	0.00213	exonic	chr21	APP	hsa-miR-4778-3p,hsa-miR-5196-3p,hsa-miR-5193,hsa-miR-877-3p,hsa-miR-103a-2-
downregulated						
hsa_circRNA_404959	10.40	0.03101	exonic	chr12	CLSTN3	hsa-miR-6848-5p,hsa-miR-6081,hsa-miR-6720-5p,hsa-miR-5591-5p,hsa-miR-6165
hsa_circRNA_047771	6.71	0.03596	exonic	chr18	NARS	hsa-miR-522-3p,hsa-miR-224-3p,hsa-miR-4677-5p,hsa-miR-140-5p,hsa-miR-153-5p
hsa_circRNA_405498	6.63	0.03760	exonic	chr16	GCSH	hsa-miR-6754-5p,hsa-miR-6812-5p,hsa-miR-5572,hsa-miR-6855-5p,hsa-miR-3612
hsa_circRNA_101408	6.45	0.04666	exonic	chr14	TTLL5	hsa-miR-136-5p,hsa-miR-500a-5p,hsa-miR-578,hsa-miR-34b-5p,hsa-miR-449c-5p
hsa_circRNA_014213	6.15	0.01028	exonic	chr1	SPRR1B	hsa-miR-6812-5p,hsa-miR-6819-5p,hsa-miR-608,hsa-miR-5572,hsa-miR-5088-5p

2 circRNA, circular RNA; PTC, papillary thyroid carcinoma; FC, fold change; Chrom: chromosome; miRNA: microRNA.

Association between hsa_circRNA_047771 and has_circRNA_007148 expression levels and clinicopathological characteristics in40 PTC patients

$^{\#}$ The mean expression value was used as the cutoff scores for the high-expression and low-expression of circRNAs. Data are expressed as n (percent) or median (interquartile range); circRNA, circular RNA; PTC, papillary thyroid carcinoma; TIRAIDS, thyroid imaging reporting and data system; TNM, tumor-node-metastasis; LNM, lymph node metastasis . * P <0.05, ** P <0.01.

1 Table 3. Association between hsa_circRNA_047771 and hsa_circRNA_007148 expression levels and
2 clinicopathological characteristics in 40 PTC patients

	hsa_circRNA_047771[#]		hsa_circRNA_007148[#]	
	High expression	Low expression	High expression	Low expression
Age(years)				
≥45	8(42.1)	13(61.9)	11(64.7)	10(43.5)
<45	11(57.9)	8(38.1)	6(35.3)	13(56.5)
Sex				
Female	14(73.7)	16(76.2)	13(76.5)	17(73.9)
male	5(26.3)	5(23.8)	4(23.5)	6(26.1)
Hashimoto				
Yes	3(15.8)	3(14.3)	2(10.5)	4(19.0)
No	16(84.2)	18(85.7)	15(88.2)	19(82.6)
TIRAIDS				
4a	2(10.5)	2(9.5)	2(11.8)	2(8.7)
4b	7(36.5)	6(28.6)	4(23.5)	9(39.1)
4c	10(52.6)	13(61.9)	11(64.7)	12(52.2)
BRAF mutation				
Yes	5(25)	12(60)*	8(47.1)	8(34.8)
No	15(75)	8(40)	9(52.9)	15(65.2)
Tumor size (cm)	1.2(0.8-2.0)	1.3(1-2.05)	1.7(1.4-2.3)	1.3(0.8-2.0)
TNM stage				
I-II	16(84.2)	9(42.9)**	7(41.2)	18(78.3)*
III-V	3(15.8)	12(57.1)	5(58.8)	10(21.7)
LNM				
Yes	7(36.8)	15(71.4)*	11(64.7)	11(48.7)
No	12(63.2)	6(28.6)	6(35.5)	12(52.2)
Focality				
Unifocal	14(73.7)	18(85.7)	11(64.7)	16(69.9)
Multifocal	5(26.3)	3(14.3)	6(35.5)	7(30.4)

3 #The mean expression value was used as the cutoff scores for the high-expression and low-expression of
4 circRNAs. Data are expressed as n (percent) or median (interquartile range); circRNA, circular RNA;
5 PTC, papillary thyroid carcinoma; TIRAIDS, thyroid imaging reporting and data system; TNM, tumor-
6 node-metastasis; LNM, lymph node metastasis. *P <0.05, **P <0.01.

Diagnostic value of circRNAs in papillary thyroid cancer.

The relative expression of each circRNA was calculated using the ΔCt method. PV, predictive value; AUC, area under the curve; CI, confidence interval.

1   Table 4. Diagnostic value of circRNAs in papillary thyroid cancer.

	hsa_circRNA_047771	hsa_circRNA_007148
Sensitivity(95% CI)	87.5(0.73-0.96)	82.5(0.63-0.97)
Specificity(95% CI)	80.0(0.64-0.91)	77.5(0.62-0.89)
+PV (95% CI)	81.4(0.66-0.92)	78.6(0.63-0.90)
-PV(95% CI)	86.5(0.71-0.96)	81.6(0.66-0.92)
Youden index	0.675	0.6
AUC(95% CI)	0.876(0.78-0.94)	0.846(0.75-0.96)

2   The relative expression of each circRNA was calculated using the ΔCt method. PV, predictive value;
3   AUC, area under the curve; CI, confidence interval.
4